Ecological Processes

RESEARCH

Open Access

Spatially explicit estimation of soil organic carbon stock of an estuarine mangrove wetland of eastern India using elemental analysis and very-fine resolution satellite data

Debajit Datta[1*], Madhumita Bairagi[1], Mansa Dey[1], Argha Pratim Pal[1] and Jibananda Gayen[1,2]

Abstract

Background: This study estimated the total soil organic C (SOC) stock of the wetland influence zone of Bichitrapur mangroves in eastern India in a spatially explicit manner. Both spatial and vertical distribution of SOC densities with respect to land use/land cover (LULC) pattern were assessed. Subsequently, some site-specific management strategies were forwarded towards enhancement of C sequestration potential.

Methods: The changing patterns of LULC within the wetland influence zone of the site were analyzed using Landsat TM (30 m) and Pleiades-1A (2 m) imageries from 1988 to 2018. Point-specific SOC measurement was done using samples taken from four core-depth intervals (viz. D1: 0–20 cm, D2: 20–40 cm, D3: 40–70 cm, D4: 70–100 cm) at 89 locations belonging to different LULC categories. Spatial interpolation was applied on this point-based data to produce SOC density and stock models as a whole and at all core-depths. Relationships between SOC density, core-depth and present LULC were evaluated through multivariate statistical analyses.

Results: The LULC transformations during last three decades suggested the gradual growth of mangrove plantations as well as agricultural and aquacultural activities. Most amount of SOC was concentrated in D1 (37.17%) followed by D3 (26.51%), while D4 had the lowest (10.87%). The highest mean SOC density was observed in the dense mangrove patches (248.92 Mg ha^{-1}) and the lowest mean was in the *Casuarina* plantations (2.78 Mg ha^{-1}). Here, Spline method emerged as the best-fit interpolation technique to model SOC data ($R^2 = 0.74$) and estimated total SOC stock of the entire wetland influence zone as 169,569.40 Mg and the grand mean as 125.56 Mg ha^{-1}. Overall, LULC was inferred as a major determinant of SOC dynamics with a statistically significant effect ($p < 0.001$), whereas no such inference could be drawn for soil core-depth.

Conclusions: The C sequestration potential of sites such as the present one could be increased with appropriate zone-wise plantation strategies, restriction on the land conversion to aquaculture and promotion of ecotourism. Periodic monitoring through integration of geospatial techniques and elemental analyses would be immensely beneficial in this regard.

Keywords: Blue C density, Core-depth, Coastal wetland, Dry combustion, Land use conversion, Wetland influence zone

*Correspondence: debajit.geo@gmail.com; debajit.datta.geog@jadavpuruniversity.in
[1] Department of Geography, Jadavpur University, Kolkata 700032, India
Full list of author information is available at the end of the article

Graphic Abstract

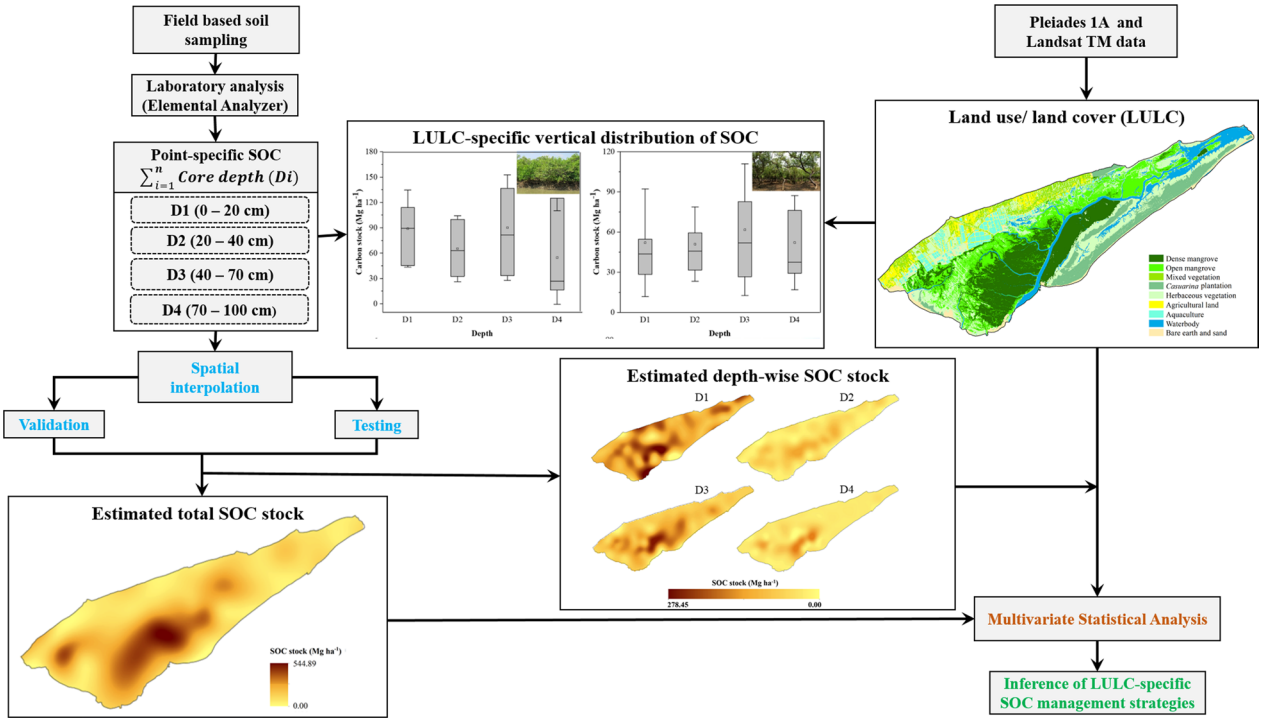

Introduction

The coastal vegetation and soils are recognized as one of the largest terrestrial pools of sequestrated carbon (C) per unit area, popularly known as the 'blue C', and thus have enormous potential to alleviate the increase of atmospheric CO_2 and conjoining greenhouse effects (Haywood et al. 2020; Yu et al. 2012). Even within the coastal environment, soil is widely considered to have relatively larger storage of C than the living vegetation and hence it is a beneficial strategy to estimate the total sequestrated blue C of the different coastal soils towards attaining an efficient management mechanism of greenhouse gases (GHGs) (Yu et al. 2012). The majority of the studies hitherto conducted on soil C had primarily focused on the C stock of the topsoil (0–20 cm) and very few have considered the deeper levels of soil at landscape level (Banerjee et al. 2020; Huo et al. 2014). However, the deeper layers of soil may have the potential to sequestrate and store high amount of C (Datta et al. 2015; Jiang et al. 2021). Thus, the C stock of deeper layers of soil needs to be included in the total soil C assessment to get a holistic picture of the sequestration potential and the available C pool of a particular landscape unit, especially the tropical coastal wetlands, such as mangroves. Most of these wetlands are fragile yet important ecosystems and excellent global blue C reserves with a potential to store almost 25% of the global soil C (Yu et al. 2012). Degradation or destruction of these wetlands would lead to augmented emissions of GHGs contributing more to climate change. Unfortunately, these ecosystems are under severe threat as human populace and development stresses in coastal regions are growing continuously (IPCC 2021). A drive to protect and restore coastal wetlands demands closer integration of these threatened land–ocean interfaces with national climate change actions and their inclusion into site-specific management initiatives. Sustainable management of coastal wetlands is particularly important in developing countries, where additional benefits from ecosystem services and products are lifelines to the local communities as highlighted in the 'United Nations Framework Convention on Climate Change' (UNFCCC) and 'Blue Carbon' management initiatives (Howard et al. 2014; UNEP 2012). In this regard, comprehensive accounting of the total soil C stocks of these coastal wetlands becomes the foremost task in accentuating their recognition as integral components of climate change mitigation strategies (IPCC 2021).

The soil C stock is influenced by many factors, such as the vegetation types, climate, hydrology, topology

and the patterns of land utilization (Bae and Ryu 2015). Evaluation of the vertical stock of C depends upon the apprehension of the spatial variability in a landscape (Dorji et al. 2014). The varying land use/land cover (LULC) patterns are key determinants of soil C, particularly of differential soil organic C (SOC) stocks (Bae and Ryu 2015). The LULC patterns play major roles in regulating the amount and quality of SOC by affecting the rates of microbial decomposition and humus stabilization, dynamics of soil physico-chemical properties, types of surface vegetation cover and expansion of built-up surfaces (Dorji et al. 2014; Guan et al. 2021). In many instances, the consideration of LULC dynamics in the assessment of SOC pools of a micro- or meso-coastal region, having same climate and soil types, becomes more imperative to gauge the levels of anthropogenic disturbances as prime drivers of regional landscape change (Guan et al. 2021; Haywood et al. 2020).

In India, comprehensive investigations on the total SOC accounting of coastal wetlands are still few and rare both spatially as well as temporally (Banerjee et al. 2020; Gnanamoorthy et al. 2019; Kandasamy et al. 2021; Mitra et al. 2011; Sahu et al. 2016). Among the few studies, majority were concerned only with point-specific measurement of mangrove soil C (Kiranmai and Sekhar 2016; Sahu et al. 2016). As per best of the knowledge of present authors, no study has been conducted yet in eastern India to measure the SOC stocks of coastal wetlands and their surroundings in a spatially explicit manner as well as assess the relationship of LULC patterns with the stocks. In view of these notable research gaps, the present study aims for a spatially explicit estimation of the total SOC stock of a mangrove wetland in an estuarine environment of eastern India through geospatial modelling of field-collected soil core sample (down to 1 m core depth) data. It further attempts to appraise in detail the effects of different LULC types and core-depths on the SOC stock of the studied wetland and its surroundings using very fine-resolution satellite imagery. Finally, this study tries to formulate customized management strategies for LULC-specific blue C management in the wetland under investigation. The mangrove plantations of Bichitrapur, Odisha and the adjoining areas under its influence within the estuarine environment of River Subarnarekha were selected as the case study site for this purpose.

Materials and methods

Description of study site

The Bichitrapur mangrove forest is extended from 87°20′58.36″E to 87°29′01.65″E and from 21°32′47.24″N to 21°37′16.77″N along the western fringe of the Medinipur Coastal Plain (MCP) and eastern side of the Subarnarekha estuary (Roy and Datta 2018). The entire MCP had developed primarily through the voluminous sedimentation of sandy, silty clayey and clayey soil particles with an underlying gravel formation during the Holocene transgression (Niyogi 1975; Chakrabarti 1995). This extensive coastal tract is characterized by wide beaches with interlinked tidal creeks, active deltas, mudflats, mangrove swamps and sand dunes (Barman et al. 2016). River Subarnarekha and other distributaries have traversed the MCP and contributed substantial amount of fresh ferruginous sediments, deposited along its western border (Chakrabarti 1995). Vegetated Chenier ridges, muddy spits, interdunal wetlands, croplands, mangrove plantations and dispersed rural settlements are certain prominent land utilization features of this area (Panda et al. 2013).

Bichitrapur had considerable amount of naturally grown littoral mangrove cover up to the 1980s (Roy and Datta 2018). However, recurring natural (viz. cyclone, sea surge and coastal erosion) and human induced disturbances (viz. wood pilferage, small-scale logging, conversion to aquaculture farms etc.) had led to severe deforestation in this area spanning from 1990s to the first decade of 21st Century. To tackle this menace, the Department of Forest and Environment (DFE), Government of Odisha, declared the area as a Proposed Reserve Forest (PRF) and raised widespread mangrove plantations around the remaining natural forest since 2008–2009 (OFSDP 2010). At present, several important species of mangroves and mangrove associates such as *Avicennia marina, Avicennia alba, Bruguiera gymnorhiza, Sonneratia apetala, Excoecaria agallocha, Pandanus tectorius, Acanthus ilicifolius* and *Porteresia coarctata* are observed throughout the PRF (Barman et al. 2019). Near the shoreline, plantations of *Casuarina equisetifolia* had established themselves over the sand ridges and dune slacks since the 1980s. Conversely, mixed stands of *Casuarina equisetifolia*, *Eucalyptus globulus, Acacia auriculiformis* and *Acacia nilotica* dominate the more inland portions of these plantations beyond the high tide line (HTL). In-between the mangrove patches and other inland tree plantations, large tracts covered with herbaceous vegetation (viz. *Sesuvium portulacastrum*, *Porteresia coarctata, Cynodon dactylon* etc.) could be found in the intertidal zone (Datta et al. 2021).

Multitudes of shrimp aquaculture farms have developed here during the last decade engulfing erstwhile fringe mangrove patches and croplands alike (Roy and Datta 2018). Hence, several parts of the study area do not represent the true mangrove wetland character at present but still these plots are under the influence of characteristic wetland eco-hydromorphology (Roy et al. 2020). It was realized during the course of this study that the greater exterior envelope of the wetland, comprising the

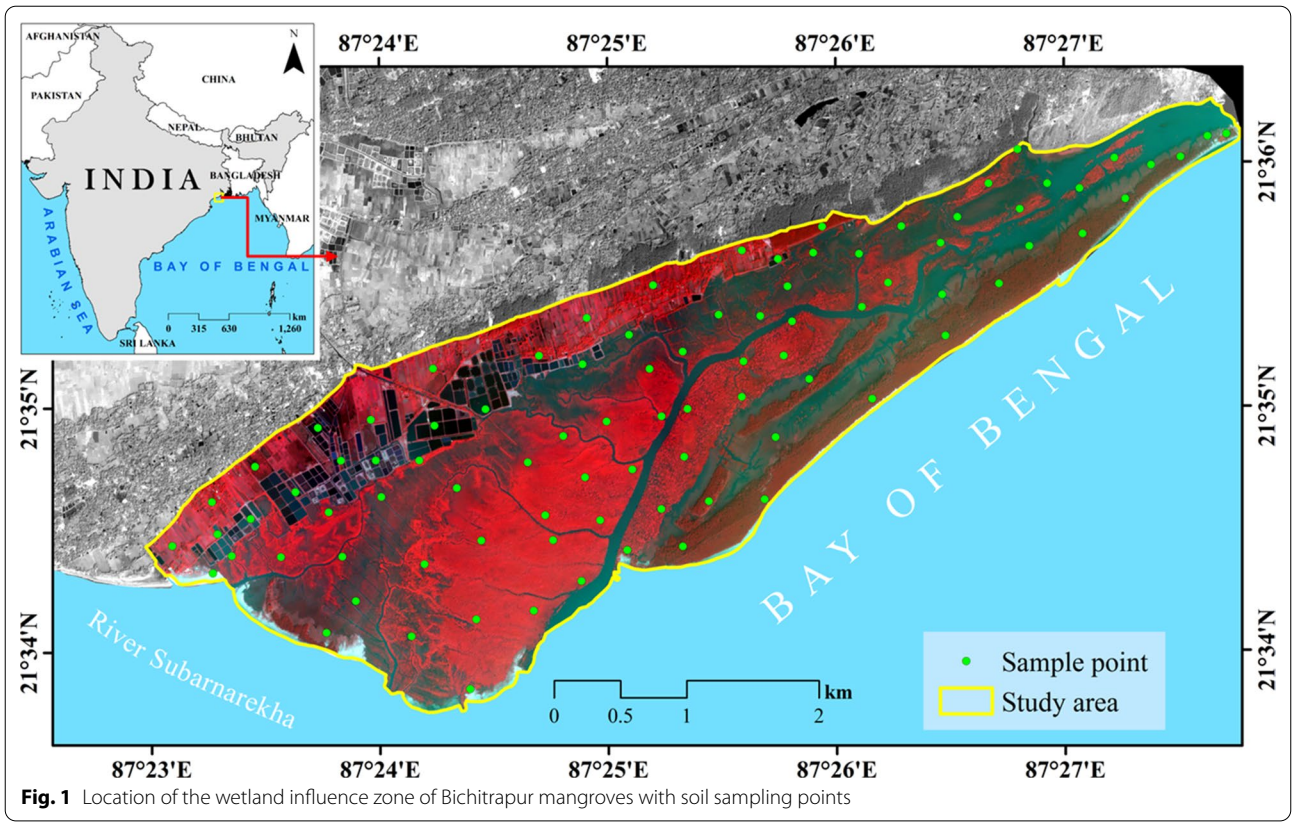

Fig. 1 Location of the wetland influence zone of Bichitrapur mangroves with soil sampling points

Table 1 Details of satellite imageries used for LULC classification

Date of Acquisition	Sensor	Path/Row	Spatial resolution (m)
17 December 1988	Landsat 5 Thematic Mapper (TM)	139/45	30
11 January 1998		139/45	
22 November 2008		139/45	
25 November 2018	Pleiades 1A	–	2

maximum area under inundation, plots of saturated surface soil during monsoon and area dominated by hydrophytes, should be considered for estimation of the total SOC stock of the site. In reality, all these plots fall within the functional boundary of the mangrove wetland (Mulamoottil et al. 1996). Accordingly, the concept of wetland influence zone (WIZ), proposed by Datta et al. (2021), had been incorporated in this study to obtain a cumulative account of total SOC stock of the study site considering both present and paleo wetland plots. Following their hybrid methodology of geospatial estimation and in-situ validation, the WIZ of Bichitrapur mangroves was delineated and it covered an area of approximately 1350.52 ha in 2020 (Fig. 1).

Land use/land cover mapping

Data source and image pre-processing

Pleiades is an environment-focused constellation consisting of two satellites with very fine-resolution multispectral sensors from *Centre National D'Études Spatiales* of France, referred to as 1A and 1B, respectively. This study used an imagery acquired by Pleiades-1A on 25 November, 2018 and supplied by the Airbus Defense and Space. The imagery includes high spatial resolution orthorectified multi-spectral data composed of four spectral bands (B: 450–530 nm; G: 510–590 nm; R: 620–700 nm; and NIR: 775–915 nm) with 2 m spatial resolution and one panchromatic band (480–820 nm) of 0.50 m resolution. The obtained Pleiades-1A imagery used in this study was already orthorectified but the locational accuracy could be improved up to 1 m using ground control points (GCPs) (Fundisi and Musakwa 2017). Hence, GCP (120 points in total) based co-registration process was carried out in February, 2019 followed by sub-setting the imagery over the delineated WIZ. Furthermore, three scenes of Landsat 5 (TM) images from 1988, 1998 and 2008 were downloaded from the open-source United States Geological Survey (USGS) website (Table 1). Atmospheric correction using Fast Line-of-sight Atmospheric Analysis of Spectral Hypercubes (FLAASH) and geometric

correction using ground control points (GCPs) were conducted over the Landsat images.

Supervised classification

The supervised classification of the obtained satellite data sets was conducted using the Support Vector Machine (SVM) algorithm. SVM is a non-probabilistic classifier that set an optimal separating hyperplane between classes to correctly separate the data point into different classes (Bai et al. 2017; Huang et al. 2002; Mountrakis et al. 2011). Through reconnaissance surveys, nine specific LULC categories were identified within the delineated WIZ, viz. (i) dense mangrove, (ii) open mangrove, (iii) mixed vegetation, (iv) *Casuarina* plantation, (v) herbaceous vegetation, (vi) agriculture, (vii) aquaculture, (viii) waterbody and (ix) bare earth and sand. The standard false colour composite (SFCC) and Google Earth geo-visualization based visual interpretation techniques coupled with field observations were applied here to manually select the training sets in the form of spectrally homogeneous polygons for each LULC class (Datta et al. 2021). These training sets were assimilated into the SVM classifier to produce the LULC maps of the study area using ENVI 5.3® image analysis software (Harris Geospatial Solutions, Broomfield, USA).

Accuracy assessment

The post-classification accuracy assessment was carried out to validate the classification outcomes and quantitatively assess how accurately pixels were classified into the corresponding LULC classes (Roy et al. 2021). Information on all the identified LULC types for 2018 were collected during the field survey from 192 in-situ data points, whereas fine resolution Google Earth images were used for collection of reference points for 1988, 1998 and 2008. Thereafter, these points were incorporated as reference points for assessing classification accuracy through computation of user's accuracy, producer's accuracy, overall accuracy and overall kappa coefficient, respectively.

Sampling design and in-situ soil sample collection

Intensive soil core sampling was carried out in February–March, 2019 using a stratified random sampling approach in which 89 soil cores were collected with respect to the various LULC categories existing within the WIZ of Bichitrapur mangroves (Mendoza-Vega et al. 2003). Sampling points were created in the ArcGIS® Pro 2.3 software (Environmental Systems Research Institute, USA) environment in such a manner so that each point should cover an approximate area of 15 ha. It was also ensured that the sampling proportions would match with the corresponding LULC proportions of the WIZ (Roy et al. 2020). Geolocations of all the sampling points were recorded by a Garmin eTrex 20x handheld device. As SOC is not distributed homogeneously in a soil profile rather changes slowly with increasing depth, the core-depths cannot be taken in equivalent intervals but need partitioning in an adequate depth-compensating manner (Kauffman and Donato 2012; Fourqurean et al. 2014). Thus, the samples were collected in four successive depth intervals of each soil core, viz. 0–20 cm (D1), 20–40 cm (D2), 40–70 cm (D3), 70–100 cm (D4), respectively, using a Russian Sediment/Peat Borer (Model 25,030, AMS Inc., Idaho, USA). However, the depths of the soil cores were limited for some sampling points due to the presence of continuous sand or gravel (non-soil) beds beyond certain depths (< 1 m). The surface soil or first depth interval of soil (D1) was collected by purposefully excluding the fresh litter layers of the sampling points, if any (Datta and Deb 2017). In this process, total 250 soil samples were collected and then analyzed for SOC estimation. To compare the SOC content of different soil depths with different intervals, it was represented with respect to per unit area, as it is the most suitable way to study the soil C content (Batjes 1996; Wuest 2009).

Laboratory analyses

The collected soil samples were dried at room temperature (25–27 °C) for a fortnight and then sieved (2 mm) as well as pulverized mechanically. Further processing and analysis of these samples were conducted in successive steps.

Estimation of point-specific bulk density

A fixed amount (50 g) of soil was measured for each sample and oven dried at 105 °C for 24 h up to a constant weight (change < 4%). The weight of the soil was then measured again and the change in weight due to moisture content loss by oven drying was noted along with the volume of dried soil (Toru and Kibret 2019). After determining the final weight of the soil and its original volume, the dry bulk density (BD) of the soil was calculated using the formula below (Dorji et al. 2014):

$$\mathrm{BD} = \frac{W_a - W_f}{V} \tag{1}$$

where W_a and W_f are the initial and final weights (g) of soil samples, respectively; V is the volume of the soil (cm^3).

Estimation of point-specific SOC stock

The SOC amount (% C_{org}) of each soil sample was determined by the dry combustion method as it provided

greater accuracy than the Loss-on-Ignition and Walkley–Black wet oxidation methods (Bhatti and Bauer 2007; Gelman et al. 2012). The Elemental C Analyzer (Flash 2000-HT, Thermo Scientific Inc., MA, USA) was used for this purpose. The SOC density of each point was further calculated as per the following equation (Fourqurean et al. 2014):

$$\text{SOC density}\left(\text{g cm}^{-3}\right) = \text{BD}\left(\text{g m}^{-3}\right) \times \left(\%C_{\text{org}}\right) \tag{2}$$

Thereafter, the amount of SOC in each core-depth interval of the soil column was determined as follows:

$$\text{SOC in core-depth}_{ij}\left(\text{g cm}^{-2}\right) = \text{SOC density}_{ij} \times \text{Core-depth interval}_{ij}(\text{cm}) \tag{3}$$

where i denotes the core-depth number of jth sample point; $i = 1, 2, 3, 4$; $j = 1, 2 \ldots n$; $n = 89$.

The amount of SOC in the entire soil core column of a specific sampling point was then measured by the following equation (Fourqurean et al. 2014):

$$\text{SOC in Soil column}_j(\text{g cm}^{-2}) = \sum_{i=1}^{4} \text{SOC in core-depth}_{ij} \tag{4}$$

Finally, the point-specific SOC of each column was represented in the standardized format of C estimation (Mg ha^{-1}) using the following conversion:

$$\begin{aligned}&\text{Point-specific SOC density}_j(Mgha^{-1})\\ &= \text{SOC in Soil column}_j(\text{g cm}^{-2}) \times \left(1Mg/1000000\,g\right)\\ &\quad \times \left(100000000\,cm^2/1\,ha\right)\end{aligned} \tag{5}$$

Spatially explicit modelling of SOC stock

The spatial modelling of SOC over the WIZ was initiated by partitioning the point-specific density data in 70:30 ratios for modeling and validation, respectively (Bhusal et al. 2018; Fidêncio et al. 2002). Various methods had been used by authors worldwide for prediction of spatial variation of soil properties that had produced differing inferences on the best performing interpolation method (Bogunovic et al. 2014; Padua et al. 2018; Robinson and Metternicht 2006; Schloeder et al. 2001; White et al. 1997; Xie et al. 2011). Based on these findings, five interpolation techniques, namely, Inverse Distance Weighting (IDW), Ordinary Kriging (OK), Radial Basis Function (RBF), Local Polynomial Interpolation and Spline were shortlisted as suitable for the present context and, accordingly, tested for spatial modelling of SOC density data using ArcGIS® Pro 2.3 software. While shortlisting, methods that do not need ancillary predictive variables (e.g., LULC pattern, elevation, soil type data etc.) were given preference as per the present research objectives. The relative effectiveness of these interpolation methods was compared through computation of the coefficient of determination (R^2) from the measured and predicted SOC values of the validation points (30% of total sampling points) (Deb et al. 2017). Ideally, coefficient of determination should be close to 1 to indicate more accurate spatial prediction. Thus, the interpolation method with best R^2 statistic was selected for the spatial modelling of SOC here.

Analysis of relationships between SOC stock, core-depth and LULC pattern

The effects of LULC categories and core-depth on the SOC densities were evaluated through statistical analyses. First, the mean (μ) and standard error (SE) values of SOC densities had beenwere computed for each core-depth interval under each LULC category. The box and whisker plots were used to represent the distribution patterns and variances of SOC densities under different LULC categories in this context due to their higher visual efficiency (Eldeiry and Garcia 2010). The statistical differences between these mean SOC values of the LULC categories were compared through one-way analysis of variance (ANOVA) with respect to each core-depth interval (Datta and Deb 2017). When ANOVA detected significant differences between mean SOC values of different LULC categories, Tukey HSD post-hoc tests (two-tailed) were conducted to analyze pairwise differences among those ($p < 0.05$, $p < 0.01$, $p < 0.001$). In addition, two-way ANOVA was also conducted to assess the individual and combined effects of core-depths and LULC categories on the mean SOC densities, respectively (Nandi et al. 2020). The mean SOC density was considered here as a dependent or response variable, whereas core-depth interval and LULC category were applied as independent control variables regulating the SOC dynamics. Finally, total SOC stocks under each LULC category as well as the whole WIZ were estimated through application of the best-fit interpolation method. Here, all statistical tests were performed using the SPSS® (Version 22.0, IBM Corporation, Armonk, USA) software.

Results

Changing LULC scenario within the WIZ

The WIZ of Bichitrapur mangroves were classified into nine LULC categories based on the ground situation of 2018–2019 (Fig. 2). Accuracy assessment of all four LULC

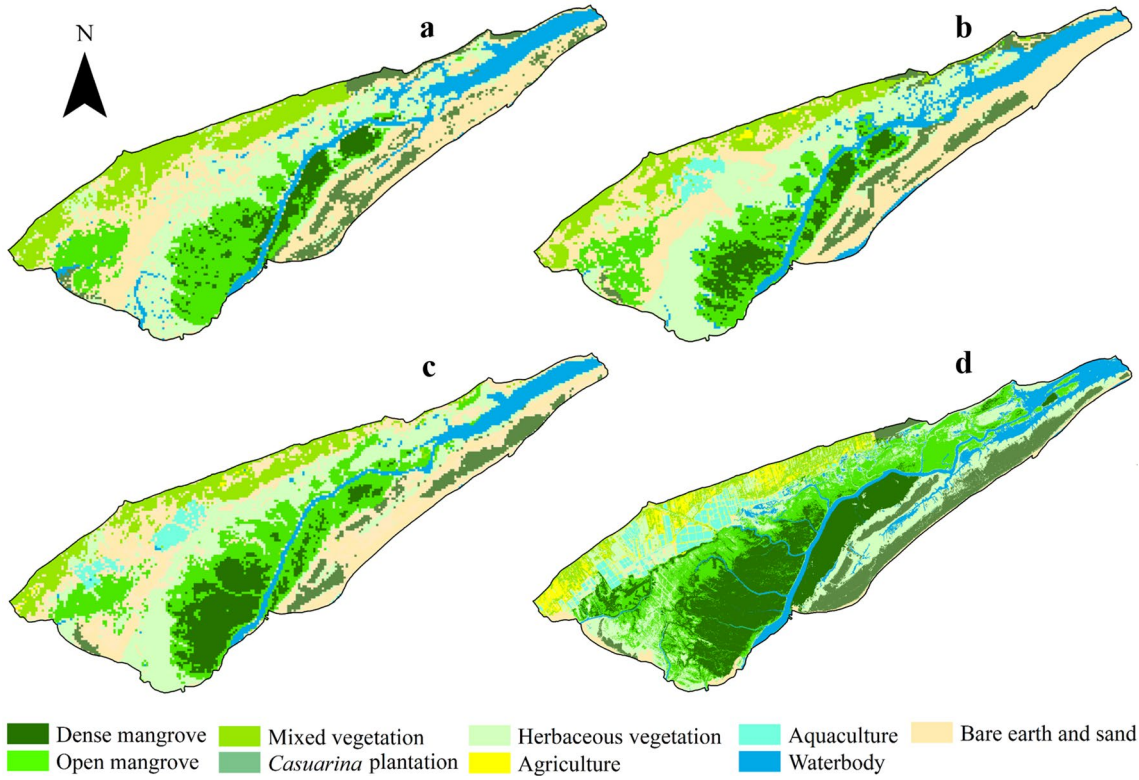

Fig. 2 Changing land use/land cover patterns of the study site from 1988 to 2018, prepared from Landsat TM and Pleiades 1A satellite imageries

maps developed in this context revealed overall accuracies of more than 80% for each assessment year (Additional file 1: Table S1). These maps showed that the entire study site had experienced notable changes in terms of LULC patterns over the last three decades (1988–2018). It witnessed an overall areal decreasing trend for mixed vegetation, bare earth and sand, and waterbody categories, while an increasing trend was observed for dense mangrove, open mangrove, *Casuarina* plantation, herbaceous vegetation, agriculture and aquaculture categories from 1988 to 2008 (Additional file 1: Table S2). Among these, although the dense mangrove category experienced a steady growth throughout, the open mangroves recorded a decrease of 1.70% only in 1998 with respect to 1988. Along with the mangroves, aquaculture category also experienced notable growth in the last three decades. *Casuarina* plantations had registered a considerable growth of 4.48% only during the last decade of assessment (2008–2018). At present, the mixed vegetation as well as the bare earth and sand categories occupy a minor area of 8.39% cumulatively, compared to the earlier 40.31% in 1988.

Among all, herbaceous vegetation covered most of the area (23.16%) followed by dense mangrove (22.71%) and open mangrove (19.51%) categories in 2018. Conversely, the bare earth and sand (3.36%), aquaculture (3.55%) and agriculture (4.03%) categories were found with least coverages (Table 5). Dense mangroves (306.73 ha) were more prevalent within the fenced zones of the PRF, whereas open mangrove patches (263.43 ha) were frequent in the fringe areas of the PRF. Outside the PRF, lesser presence of agriculture was a notable departure from the regional LULC pattern and could be attributed to the recent growth of shrimp aquaculture (47.93 ha) and farm-forestry (mixed vegetation patches: 5.03%) activities through conversion of erstwhile paddy dominated croplands at this site. The proportion of land area under *Casuarina* plantation (9.71%) was relatively higher along the shoreline. Waterbodies (8.94%) within the WIZ primarily comprised of the river channel, tidal creeks and other naturally waterlogged areas. Land area under the bare earth and sand category (45.33 ha) were greater along the shoreline than the inland parts chiefly due to the presence of bare mudflats and sandy beaches.

Distribution patterns of SOC stock

Vertical distribution of SOC

Laboratory based analyses of soil core samples revealed that the vertical distribution of SOC contents varied across core-depths (Table 2). Among the core-depth intervals, the D3 ($\bar{x} = 56.04$ Mg ha^{-1}) interval represented highest

Table 2 Mean SOC densities (Mg ha^{-1}) with standard error (± SE) values for the successive core-depth intervals of the soils within the WIZ. *n* = number of samples collected at varying core-depths

Depth	*n*	D1 [0–20 cm]	*n*	D2 [20–40 cm]	*n*	D3 [40–70 cm]	*n*	D4 [70–100 cm]
SOC stock	89	49.44 ± 4.75	74	40.72 ± 4.18	56	56.04 ± 7.47	32	40.22 ± 7.32

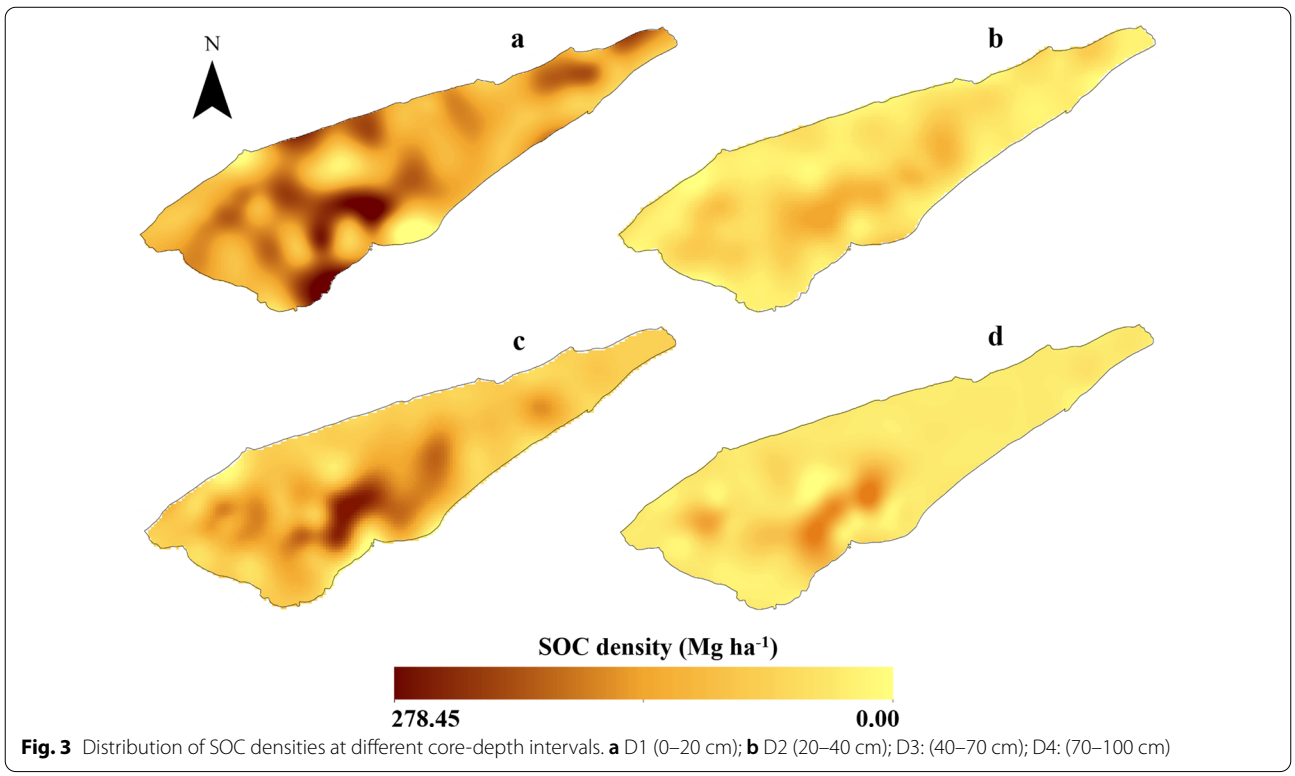

Fig. 3 Distribution of SOC densities at different core-depth intervals. **a** D1 (0–20 cm); **b** D2 (20–40 cm); D3: (40–70 cm); D4: (70–100 cm)

mean value of SOC density while D4 ($\bar{x}$ = 40.22 Mg ha^{-1}) was the lowest. The D1 ($\bar{x}$ = 49.44 Mg ha^{-1}) and D2 ($\bar{x}$ = 40.72 Mg ha^{-1}) were measured to have intermediate amounts of SOC (Fig. 3). Here, the total SOC density was found to be highest at D1 (4400.52 Mg ha^{-1}, 37.17% of site total) and lowest at D4 (1287.19 Mg ha^{-1}, 10.87%). Even also under this context, D3 (3138.08 Mg ha^{-1}, 26.51%) showed larger amount than that of D2 (3012.93 Mg ha^{-1}, 25.45%), indicating towards higher rates of C sequestration at this site in the geologic past. This pattern was most evident in case of mixed vegetation category, in which highest SOC concentration was found at D3 (31%). However, this should be noted that the D3 and D4 intervals were not at all observed in many instances, specifically under the bare earth and sand, *Casuarina* plantation, and agriculture categories, respectively.

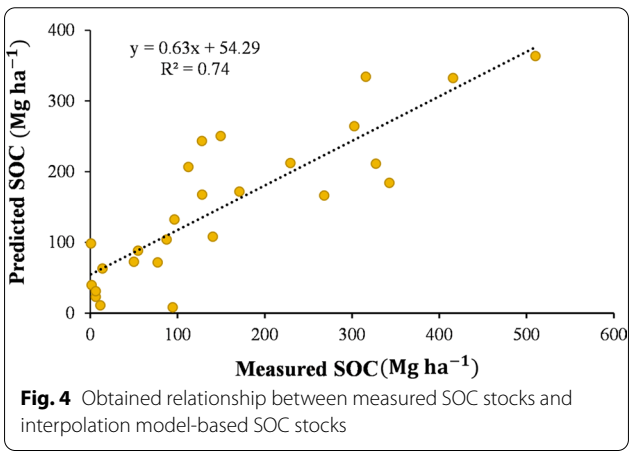

Fig. 4 Obtained relationship between measured SOC stocks and interpolation model-based SOC stocks

Performance of spatial interpolation methods

The accuracies of spatially predicted SOC values using five different spatial interpolation methods were assessed through computation of their respective R^2 values (Table 3). Among all, the Spline (R^2 = 0.74) method showed the best

Table 3 Coefficient of determination (R^2) estimated for different spatial interpolation methods with respect to the relationship between the observed and corresponding predicted SOC values

Method of interpolation†	Reference	Value of R^2 obtained in this study
IDW	Padua et al. 2018; Robinson and Metternicht 2006	0.65
OK	Bhusal et al. 2018; Robinson and Metternicht 2006	0.45
RBF	Fidêncio et al. 2002	0.67
LPI	Bogunovic et al. 2014; White et al. 1997; Xie et al. 2011	0.72
Spline	Bhusal et al. 2018; Schloeder et al. 2001	0.74

† IDW Inverse Distance Weighting, *OK* Ordinary Kriging, *RBF* Radial Basis Function, *LPI* Local Polynomial Interpolation

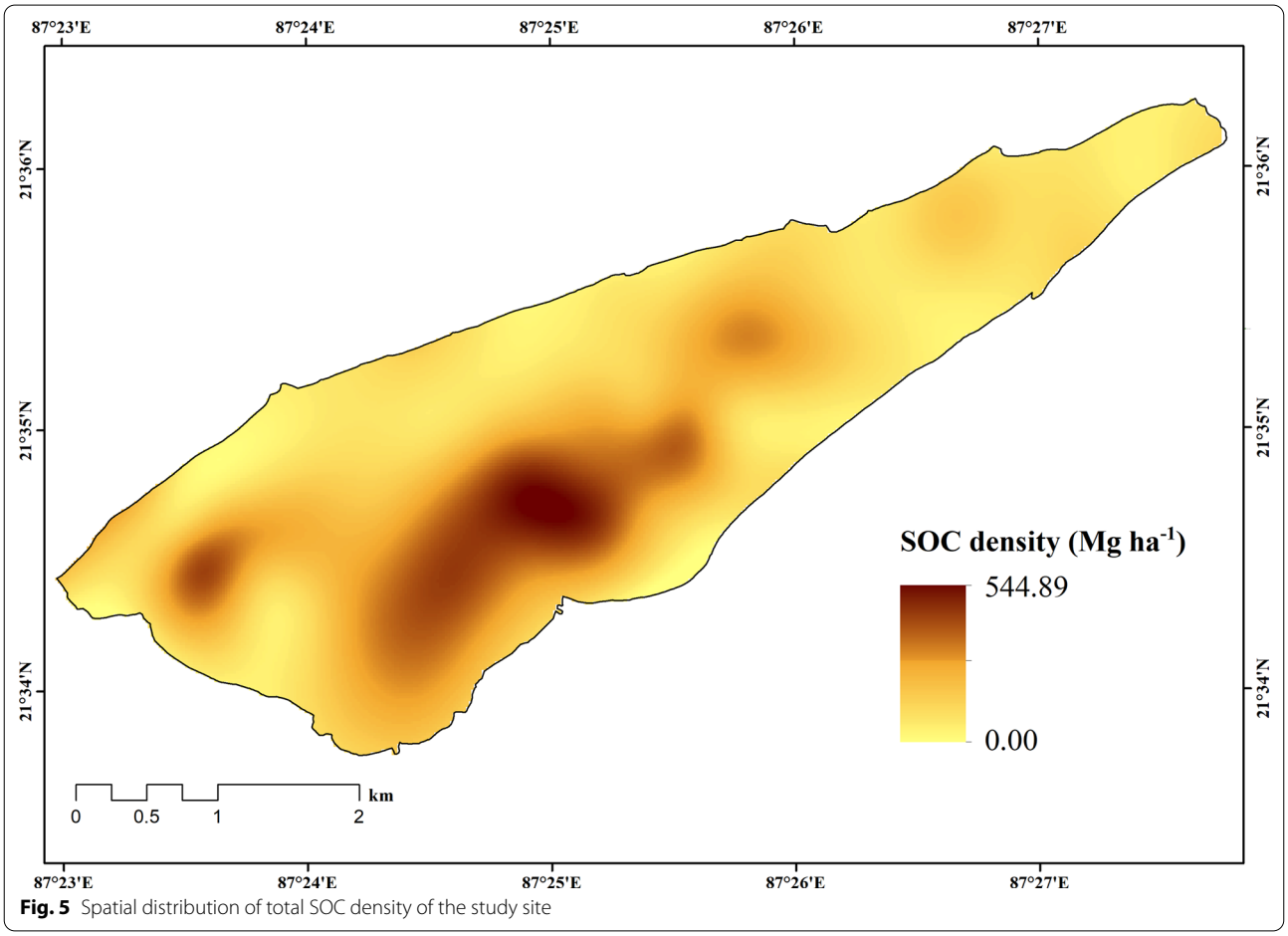

Fig. 5 Spatial distribution of total SOC density of the study site

fit followed by Local Polynomial Interpolation ($R^2 = 0.72$). The validation results were also checked through bi-axial scatter graphs fitted with regression trend lines (Fig. 4). Accordingly, the Spline method was used further for the spatially explicit modelling of total SOC stock in the WIZ from the point-specific sample data. It was also applied to prepare the depthwise spatial distribution maps of SOC pools.

Horizontal trend of SOC densities

The spatially predicted SOC densities of the study site revealed wide variations, ranging from almost zero to 544.89 Mg ha^{-1}. In general, the higher amount of SOC

Table 4 Mean ($\bar{x}$) SOC densities with standard error (± SE) values across different LULC categories and soil core-depths[†]

LULC category	SOC density (Mg ha^{-1})							
	D1		D2		D3		D4	
	n	$\bar{x}$ ± SE	*n*	$\bar{x}$ ± SE	*n*	$\bar{x}$ ± SE	*n*	$\bar{x}$ ± SE
Dense mangrove	23	89.00 ± 9.53^{A}	23	65.25 ± 8.12^{A}	18	90.22 ± 14.72^{A}	10	54.70 ± 17.51
Open mangrove	17	52.01 ± 9.73^{B}	17	50.91 ± 6.72^{AC}	17	$61.70 \pm 11.92^{A,B}$	11	52.10 ± 10.58
Mixed vegetation	4	5.25 ± 0.14^{BC}	4	4.20 ± 0.44^{BC}	4	5.77 ± 0.28^{B}	3	4.51 ± 0.73
Casuarina plantation	8	2.41 ± 0.94^{C}	1	2.93 ± 0.00^{C}	NA	NA	NA	NA
Herbaceous vegetation	18	40.16 ± 7.88^{BC}	16	19.13 ± 5.68^{B}	10	12.40 ± 3.04^{B}	5	18.41 ± 7.07
Agriculture	4	8.26 ± 4.72^{BC}	4	3.29 ± 0.53^{BC}	1	4.24 ± 0.00^{C}	NA	NA
Aquaculture	6	66.50 ± 14.43^{AB}	6	39.43 ± 11.72	4	$61.19 \pm 30.78^{A,B}$	2	28.37 ± 21.17
Waterbody	5	45.61 ± 8.97	3	23.78 ± 8.18	2	$34.56 \pm 11.52^{A,B}$	1	4.77 ± 0.00
Bare earth and sand	4	11.53 ± 0.41^{BC}	NA	NA	NA	NA	NA	NA
Multivariate analysis	*df*			8, 3, 18				
	LULC category			11.15***				
	Core-depth			1.52				
	LULC category × core-depth			0.50				

[†] Soil samples were collected at varying core-depth intervals of D1 = 0–20 cm; D2 = 20–40 cm; D3 = 40–70 cm; and D4 = 70–100 cm. *n* number of samples for each LULC category at a particular depth; NA = data unavailable due to absence of soil layer at a particular depth under any LULC category. Different superscript letters represent significant differences among LULC categories at a particular core-depth according to one-way ANOVA (*F*) followed by Tukey HSD Post Hoc test at $p < 0.05$. Significance values of two-way ANOVA (*F*) for comparisons of individual and combined effects of LULC category and core-depth on SOC density. Degrees of freedom are represented by *df*. Levels of significance are shown as: ***$p < 0.001$

pools (>300 Mg ha^{-1}) was mostly traced along the tidal creeks and river channel within the dense and open mangrove patches. Majority of these patches were found to be part of the PRF during ground truthing. In contrast, a secondary zone of large SOC pool (>270 Mg ha^{-1}) was identified in the north-western corner of the WIZ (Fig. 5). In reality, this zone was outside the ambit of the PRF and found within community-owned plots. It primarily had a mixed LULC pattern comprised of aquaculture, dense mangrove and open mangrove categories. Overall, the highest SOC density (544.89 Mg ha^{-1}) was obtained in a dense mangrove zone, while the lowest amount (almost 0.00 Mg ha^{-1}) was predicted for the south-central portions of the *Casuarina* plantation along the shoreline. The model revealed that almost 46% of the total WIZ area had SOC densities of more than 200 Mg ha^{-1}, whereas 32% of the area was consisted of moderate SOC pools (100–200 Mg ha^{-1}). The remaining 22% of WIZ area was estimated to have lower amounts of SOC (<100 Mg ha^{-1}).

Effects of LULC pattern and core-depth on SOC stock

SOC densities of the WIZ of Bichitrapur mangroves were highly variable among areas under the different LULC categories in 2018. These differences were examined in detail with respect to the four core-depth intervals considered in this study (Table 4). In D1, very high SOC concentrations were found in dense mangrove ($\bar{x}$ = 89.00 Mg ha^{-1}), open mangrove ($\bar{x}$ = 52.01 Mg ha^{-1}), herbaceous vegetation ($\bar{x}$ = 40.16 Mg ha^{-1}), aquaculture ($\bar{x}$ = 66.50 Mg ha^{-1}) and waterbody ($\bar{x}$ = 45.61 Mg ha^{-1}) categories. On the contrary, lower SOC densities were recorded in mixed vegetation ($\bar{x}$ = 5.25 Mg ha^{-1}), *Casuarina* plantation ($\bar{x}$ = 2.41 Mg ha^{-1}), agriculture ($\bar{x}$ = 8.26 Mg ha^{-1}), and bare earth and sand ($\bar{x}$ = 11.53 Mg ha^{-1}) covered areas. Statistically, the dense mangrove soil had significant difference of mean SOC density with all other categories ($p < 0.05$) except those of aquaculture and waterbody.

Regarding D2, the previous sequence of LULC categories with respect to SOC densities changed slightly as open mangrove ($\bar{x}$ = 50.91 Mg ha^{-1}) emerged as the second highest one replacing the aquaculture ($\bar{x}$ = 39.43 Mg ha^{-1}) category. Here, six out of the total nine LULC categories depicted notably poor SOC concentrations ($\bar{x}$ < 25 Mg ha^{-1}). Accordingly, the dense mangrove category showed significant differences with all other LULC categories except the open mangrove in this depth interval ($p < 0.05$). Notably, this core-depth of open mangrove had the presence of almost a same percentage of total SOC stock (23.49%) as the first one, whereas for the dense mangrove, the amount was far lesser in D2 (20,014.13 Mg) than in D1 (27,298.97 Mg). The SOC in D2 of herbaceous vegetation was significantly lower than its D1 (Fig. 6).

The sequence of LULC categories observed for D1 almost matched with that of D3, as aquaculture regained the second spot following dense mangrove. For mixed

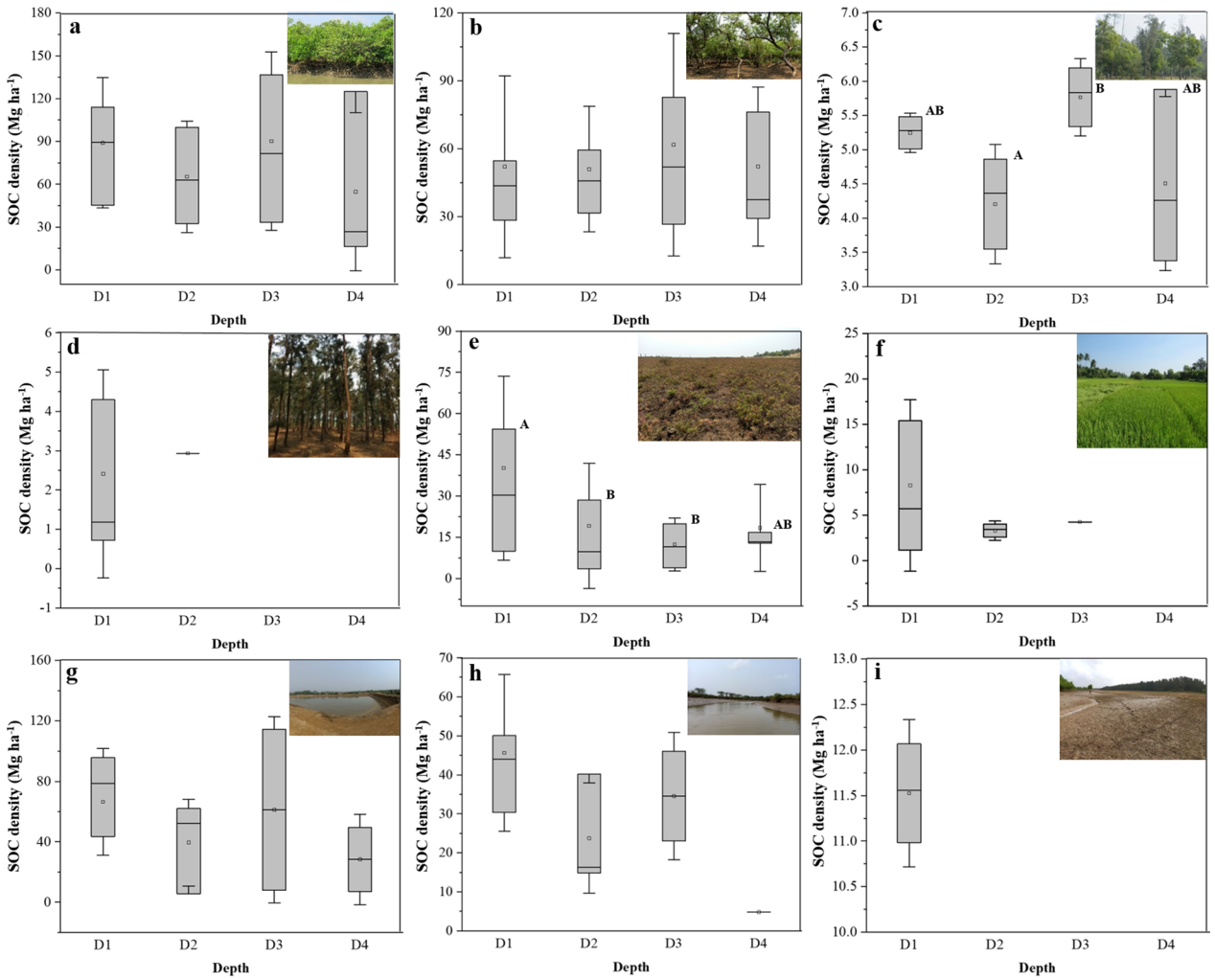

Fig. 6 SOC densities of the four core-depth intervals under different LULC categories. **a** dense mangrove; **b** open mangrove; **c** mixed vegetation; **d** *Casuarina* plantation; **e** herbaceous vegetation; **f** agriculture; **g** aquaculture; **h** waterbody; **i** bare earth and sand. Different superscript letters represent significant differences among core-depth intervals under a particular LULC category according to one-way ANOVA (*F*) followed by Tukey HSD Post Hoc test at $p < 0.05$

vegetation, there was significant difference of SOC between D2 and D3 ($p < 0.05$). This depth layer was conspicuously absent for the *Casuarina* plantation as well as bare earth and sand categories, hence these categories were omitted from further consideration in this particular assessment. Among the rest of the categories, agriculture was most distinctively as well as significantly different ($p < 0.05$) from others due to its notably poor SOC density at this depth ($\bar{x} = 4.24$ Mg ha^{-1}). In reality, plots under agriculture category were mostly found only down to the D2 depth throughout the WIZ. Remarkably, the mean SOC densities and total stocks of D3 for most of the LULC categories were higher than those of D2.

In D4, wide variations among point-specific samples were recorded across LULC categories, as indicated by their respective large SE values. Thus, although the generally observed sequence of decreasing mean SOC densities for different LULC categories was almost maintained in this depth layer with the sole exception of aquaculture (lower than open mangrove), no statistically significant difference among these values could be deduced ($p > 0.05$). Along with the complete absence of soil under agriculture, *Casuarina* plantation, bare earth and sand categories, most plots under aquaculture and waterbody were also devoid of this depth layer, as evident from their very low sample sizes in this case ($n < 3$).

Table 5 Estimated total SOC stocks and mean, minimum, maximum and standard error (SE) values of SOC densities under different LULC categories

LULC category	Area (ha)	Area (%)	Total SOC stock (Mg)	Mean SOC (Mg ha^{-1})	Minimum SOC (Mg ha^{-1})	Maximum SOC (Mg ha^{-1})	SE (Mg ha^{-1})
Dense mangrove	306.73	22.71	76,351.16	248.92	68.60	544.89	22.88
Open mangrove	263.43	19.51	52,247.13	198.33	54.35	523.28	28.45
Mixed vegetation	67.89	5.03	1262.37	18.59	0.00	39.07	1.79
Casuarina plantation	131.20	9.71	364.09	2.78	0.00	11.53	1.20
Herbaceous vegetation	312.82	23.16	21,635.05	69.16	5.69	156.34	11.44
Agriculture	54.43	4.03	686.08	12.60	4.82	58.28	4.23
Aquaculture	47.93	3.55	7485.66	156.18	36.57	326.17	44.04
Waterbody	120.76	8.94	9015.39	74.66	19.69	141.75	15.33
Bare earth and sand	45.33	3.36	522.47	11.53	0.00	17.08	0.41
Total	1350.52	100.00	169,569.40	125.56	0.00	544.89	-

Regarding the total SOC stock, the following descending order was obtained: dense mangrove (76,351.16 Mg) > open mangrove (52,247.13 Mg) > herbaceous vegetation (21,635.05 Mg) > waterbody (9015.39 Mg) > aquaculture (7485.66 Mg) > mixed vegetation (1262.37 Mg) > agriculture (686.08 Mg) > bare earth and sand (522.47 Mg) > *Casuarina* plantation (364.09 Mg) (Table 5). Thus, the total SOC stock of the entire WIZ of Bichitrapur mangroves was estimated as 169,569.40 Mg. However, the order of LULC categories based on mean SOC densities of all depths was as follows: dense mangrove > open mangrove > aquaculture > waterbody > herbaceous vegetation > mixed vegetation > agriculture > bare earth and sand > *Casuarina* plantation. This difference between the two orders of decreasing SOC amounts could be attributed chiefly towards the varied areal coverages of different LULC categories within the WIZ. Overall, aquaculture plots recorded highest variance among its predicted values followed by open mangroves. Moreover, it could be inferred from the study that for different core-depth intervals, similar SOC densities were found, whereas for any particular core-depth under different LULC categories, different SOC densities were obtained. These inferences were also evidenced from the two-way ANOVA, which revealed a statistically significant effect of LULC category on SOC density ($p < 0.001$), making it a major determinant of SOC dynamics. Conversely, neither soil core-depth individually nor core-depth and LULC jointly was found as significant controlling factor(s) of the SOC density as a whole ($p > 0.05$).

Discussion

LULC as a driver of spatial heterogeneity in SOC stock

Rate of SOC sequestration is a function of the combined actions of climate, vegetation type, topography and soil type (Haywood et al. 2020; Mendoza-Vega et al. 2003). In a coastal wetland environment, such as the present study site, the pattern and duration of inundation and rate of removal of freshly fallen litter through run-off also have considerable effects on SOC dynamics (Datta and Deb 2017; Yu et al. 2012). LULC patterns often act as the proxy of vegetal cover and exert influence on the rates of soil organic matter accumulation and SOC mineralization, thereby controlling SOC accumulation (Bae and Ryu 2015). The effects of existing LULC pattern and their transformation scenarios become even more influential if the studied wetland site constitutes a small landscape unit (< 1500 ha) and is under the same climate, broad soil type and topography, which is the case here (Yu et al. 2012). Acknowledging the due importance of LULC pattern on the SOC stock, we conducted the present investigation with very fine-resolution Pleiades-1A imagery.

Wetlands such as the Bichitrapur mangroves, having high vegetation productivity as well as low decomposition rate of C, generally represent high amount of SOC stock (Mou et al. 2018). This fact is evident from the higher SOC concentrations ($\bar{x} > 190$ Mg ha^{-1}) in dense and open mangrove patches of this site and could be attributed to the accumulation of larger aboveground and belowground biomass contents in an anaerobic condition for prolonged time. Conversely, the lower SOC concentrations ($\bar{x} < 70$ Mg ha^{-1}) in herbaceous vegetation and agriculture categories could be attributed to the limited potential of C inputs in the soil from relatively lesser aboveground biomass. However, these mean values should be considered with respect to their corresponding sample sizes only, as the sizes decreased gradually with increasing depth from the surface. In this regard, the total SOC stocks in each core-depth across the WIZ, calculated based on point-specific sampling, might provide a clearer picture of C dynamics. The SOC content of agricultural land (686.08 Mg) seemed to be very low

which might be the combined effect of intensive farming, unscientific ways of crop harvesting and soil tillage practices and uncontrolled application of chemical fertilizers (Guan et al. 2021; Roy and Datta 2018). Nevertheless, the presence of excessive sand deposits at near-surface soil layers was found to be one of the prime determinants of lower SOC concentrations ($\bar{x} < 20$ Mg ha^{-1}) in agriculture (at some plots near shoreline), mixed vegetation, *Casuarina* plantation and bare earth and sand categories. This sandy soil at the surface (D1) and only sand just below D2 or D3 intervals actually resulted into exceptionally low amount of organic matter and thereby very poor amount of SOC under these LULC categories. Besides, the bare earth and sand covered plots had very low amount of SOC primarily due to the absence of any vegetation cover. Some of the bare earth plots were in a transitional stage from open mangrove or agriculture to aquaculture farms and thus were the evidences of rampant small-scale deforestation and LULC conversion continuing in this part of eastern India (Roy et al. 2021).

Apparently, lentic characteristic, different artificial fish feeds, chemical fertilizers and manures used in aquaculture as well as decomposed dead bodies and excrements of aquatic animals had led towards the high SOC concentration in aquaculture farms (Roy et al. 2021). However, the influence of paleo-land covers should not be overlooked in this context, since many of the aquaculture plots had gone through successive stages of LULC transformation during the last 50 years, mostly in the following sequence: mangrove – bare earth – agriculture – bare earth – aquaculture (Roy and Datta 2018). Thus, the relatively higher level of mean SOC density ($\bar{x} = 61.19$ Mg ha^{-1}) at D3 of aquaculture category might be related to the former mangrove vegetation cover of these plots. Similarly, the mean SOC concentration of the bare earth and sand category at D1 was considerably higher than the amounts of mixed vegetation, agriculture and *Casuarina* plantations. This higher concentration of SOC in some 'bare earth' plots probably indicated towards the recent occurrence of deforestation, where vegetation covers existed in the past. Nevertheless, as many farmers of this site were found to be willing to convert their sandy soil dominated croplands to aquaculture farms chiefly owing to the prospect of rapid as well as higher monetary returns, area under aquaculture would surely increase in near future. The patterns of LULC transformation of this site in the last 30–40 years, as revealed in this study, also supported this trend. However, the SOC density might not show any notable growth due to this specific conversion process. On the contrary, the general lotic characteristic of the waterbodies within the WIZ decelerated the sedimentation process, thereby leading towards low to medium amounts of SOC concentration (Overall $\bar{x} = 74.66$ Mg ha^{-1}) there.

In the current study, the highest SOC stock for mangrove region was found within upper part (20 cm) of the soil profile and somewhat lesser in the deeper section. This contradicted the trend for mangrove soils of several part of India. For example, highest concentration of SOC was found within the depth of 16–30 cm and comparably lower in the upper layer (0–15 cm) in Gujarat (Pandey and Pandey 2013). This contrasting scenario also prevailed in the Bhitarkanika Conservation Area of Odisha, where the highest amount of SOC stock was recorded below 100 cm of depth for mangroves (Bhomia et al. 2016). However, the estimated SOC pool (40–70 cm) for aquaculture in this study is comparable with that of Bhitarkanika (50–100 cm) (Bhomia et al. 2016). Similarly, the mangrove sites of Vellar estuary showed a similar trend of decreasing SOC with increasing depth (Kathiresan et al. 2014). The estimated SOC stock of mangroves here is higher compared to the mangroves of Kerala for the depth of 60 cm and highest concentrations were recorded for the upper layer of 0–45 cm (Harishma et al. 2020; Rani et al. 2021). The estimated SOC density is also higher than both the plantations and natural mangroves of Mahanadi estuary of Odisha but notably lower than that of Sundarbans of West Bengal (Mitra and Banerjee 2012; Sahu et al. 2016). This difference might be due to Bichitrapur being a recent plantation, while Sundarbans is a natural mangrove forest. In addition, the rate of SOC mineralization is also a predominant factor of soil organic matter decomposition (Ross et al. 1999). Any change in the rate of SOC mineralization resulting from human interventions thus have the potential to alter SOC storage in wetland environments (Mou et al. 2018; Wang et al. 2014). It was evident from the present study that the SOC stocks were notably lower in lands with more human induced disturbances than those with natural wetland vegetation. For example, the dense and open mangrove patches, being relatively undisturbed, accumulated higher amount of SOC pools but the plots under agriculture, bare earth, waterbody etc. contain much lower amounts. Therefore, incessant conversion of wetland areas to croplands and aquaculture farms poses a severe threat to the regional environmental sustainability through considerable reduction of the current C sequestration potential of the study site.

Site-specific strategies of SOC management

The WIZ of Bichitrapur mangroves recorded a relatively lower SOC density ($\bar{x} = 125.56$ Mg ha^{-1}) than other similar mangrove wetlands of South and Southeast Asia such as the Chek Jawa in

Singapore (497 Mg ha^{-1}), Jakarta Bay in Indonesia (531.53 Mg ha^{-1}) and Batticaloa lagoon in Sri Lanka (1009 Mg ha^{-1}) (Jonsson and Hedman 2018; Phang et al. 2015; Slamet et al. 2020). There were several reasons of this low amount of sequestrated C in this site. Even after considering the fact that the entire WIZ did not only have the actual mangrove patches but also other partially or fully humanized LULC categories (viz. aquaculture, *Casuarina* plantation, agriculture and bare earth), the total SOC stock could be considered as very poor under the perfect tropical estuarine geo-environmental conditions present there (Roy et al. 2020). These low values were also due to the faulty plantation strategies implemented in this site with respect to mangroves and other coastal vegetation (Datta et al. 2021). Thus, it was realized from the study that there is sufficient scope of enhancing the C sequestration capacity of the WIZ, provided integrated coastal management initiatives are implemented appropriately. The DFE has already implemented ecotourism initiatives here and it could become fruitful in managing this fragile wetland site. In this regard, some site-specific conservation and management measures are formulated based on the experience of the present study. These are as follows: (1) sincere efforts should be made by the DFE to bring this site under the globally recognized 'Reducing Emissions from Deforestation and Forest Degradations and the role of conservation, sustainable management of forests and enhancement of forest carbon stocks in developing countries' (REDD +) programme for obtaining necessary funding for mangrove management (MoEF and CC 2018); (2) Possible inclusion of privately owned barren lands and bare mudflat areas under the ambit of mangrove plantation; (3) Mangrove species known for their erosion-resistance as well as C sequestrating potentials (viz. *Avicennia* varieties, *Excoecaria agallocha, Rhizophora mucronata* and *Porteresia coarctata*) should be prioritized for plantation along the shoreline; (4) In the interiors of the PRF, *Bruguiera gymnorhiza, Ceriops* varieties, *Nypa fruticans* and *Sonneratia apetala* might be given priority; (5) Large shrimp monoculture farms should be regulated within the WIZ through introduction of a land ceiling and, at the same time, smallholder based integrated mangrove-shrimp farming practices should be encouraged.

Conclusions

The present study provided comprehensive analysis of spatial variability of SOC stocks as well as their concentrations across different LULC categories of the WIZ of Bichitrapur mangroves. The findings revealed a general trend of higher SOC densities in D1 and D3 core-depth intervals. Conversely, the SOC density values were relatively lower in D2 and D4 intervals. Overall, high SOC concentrations were observed in dense mangrove, open mangrove and aquaculture areas, while the other LULC categories recorded low SOC concentrations. Some necessary management strategies to enhance the SOC sequestration potential of the study site were also devised in this research work. Although the study could be envisaged as a pioneering approach in soil blue C estimation in this part of India through integration of 'state of the art' elemental analyses and very-fine resolution satellite imagery based geospatial modelling, it also had few limitations. First, the use of different explanatory covariates, such as detailed soil map, soil mineralogical variation, micro-topographic etc., could not be used to increase the accuracy of SOC estimation (e.g., use of Regression Kriging) owing to data unavailability at the appropriate spatial scale. In addition, the SOC stock was estimated down to 1 m from the surface, whereas in some cases, there might be soil layer beyond that depth. Lastly, assessment of temporal changes of past SOC densities was not possible due to the absence of affordable fine resolution imagery (~2 m) before 2011 as well as archival point-specific SOC data of this region. Hence, the future research in this context should include multi-temporal LULC data set, entire soil profile-based C data and sophisticated covariate-based interpolation technique towards more accurate and periodical monitoring. Based on the findings of such continuous monitoring, sustainable management of these sorts of small tropical coastal wetlands as effective sinks of blue C could be attained and, thereby channelized towards the mitigation of global climate change.

Abbreviations

GHG: Greenhouse gas; SOC: Soil organic carbon; LULC: Land use/land cover; MCP: Medinipur Coastal Plain; WIZ: Wetland influence zone; DFE: Department of Forest and Environment, Government of Odisha; PRF: Proposed reserve forest; CNES: *Centre National D'Études Spatiales*; NIR: Near-infrared; GCP: Ground control point; SVM: Support vector machine; IDW: Inverse distance weighting; OK: Ordinary kriging; RBF: Radial basis function; LPI: Local polynomial interpolation; RMSE: Root mean square error; REDD +: Reducing Emissions from Deforestation and Forest Degradations and the role of conservation, sustainable management of forests and enhancement of forest carbon stocks in developing countries.

Supplementary Information

The online version contains supplementary material available at https://doi.org/10.1186/s13717-022-00370-4.

Additional file 1: Table S1. Accuracy assessment of supervised classifications of satellite imageries used in the study. **Table S2.** LULC statistics of the study site from 1988 to 2018.

Acknowledgements
We are thankful to the local coastal community members for their assistance during field investigations. We acknowledge the financial assistance provided by the Science and Engineering Research Board, Department of Science and Technology (DST-SERB), Government of India, to the Corresponding author.

Authors' contributions
DD, MB, and MD conceptualized and designed the research. APP and MB performed the elemental analyses. Spatial modelling was done by DD and MD. Statistical analyses were conducted by DD and JG. All authors contributed equally to the interpretation and discussion of the results. DD and MB wrote the first draft and all other authors read, revised, and approved the final manuscript. All authors read and approved the final manuscript.

Funding
This research work is conducted with the financial support received by the corresponding author from the Science and Engineering Research Board, Department of Science & Technology (DST-SERB), Government of India (SERB Sanction No. ECR/2017/003380, dated November 26, 2018).

Availability of data and materials
The data sets used and/or analyzed during the current study are available from the corresponding author on reasonable request.

Declarations

Ethics approval and consent to participate
Not applicable.

Consent for publication
Not applicable.

Competing interests
The authors declare that they have no competing interests.

Author details
[1]Department of Geography, Jadavpur University, Kolkata 700032, India.
[2]Department of Geography, Sree Chaitanya College, Habra 743268, India.

Received: 20 October 2021 Accepted: 3 March 2022
Published online: 27 March 2022

References

Bae J, Ryu Y (2015) Land use and land cover changes explain spatial and temporal variations of the soil organic carbon stocks in a constructed urban park. Landsc Urban Plan 136:57–67
Bai X, Sharma RC, Tateishi R, Kondoh A, Wuliangha B, Tana G (2017) A detailed and high-resolution land use and land cover change analysis over the past 16 years in the Horqin sandy land, Inner Mongolia. Math Probl Eng. https://doi.org/10.1155/2017/1316505
Banerjee K, Sahoo CK, Bal G, Mallik K, Paul R, Mitra A (2020) High blue carbon stock in mangrove forests of Eastern India. Trop Ecol 61:150–167. https://doi.org/10.1007/s42965-020-00072-y
Barman NK, Chatterjee S, Paul AK (2016) Coastal morphodynamics: integrated spatial modeling on the deltaic Balasore coast, India. Springer Nature, Switzerland
Barman NK, Paul AK, Maity M, Pahari S (2019) Mangrove species succession and zonation pattern estimation in relation with landscape characteristics through quadrate method at Bichitrapur Mangroves, Odisha. J Coast Sci 7:1–7
Batjes NH (1996) Total carbon and nitrogen in the soils of the world. Eur J Soil Sci 47:151–163. https://doi.org/10.1111/j.1365-2389.1996.tb01386.x
Bhatti JS, Bauer IE (2007) Comparing loss-on-ignition with dry combustion as a method for determining carbon content in upland and lowland forest ecosystems. Commun Soil Sci Plant Anal 33:3419–3430. https://doi.org/10.1081/CSS-120014535
Bhomia RK, MacKenzie RA, Murdiyarso D, Sasmito SD, Purbopuspito J (2016) Impacts of land use on Indian mangrove forest carbon stocks: implications for conservation and management. Ecol Appl 26:1396–1408
Bhusal B, Lamichhane S, Shrestha RK (2018) Maping the soil fertility of Bisankhel Catchment of Chitlang VDC and comparison of different geospatial interpolation techniques. J Inst Agric Anim Sci 35:95–104. https://doi.org/10.3126/jiaas.v35i1.22519
Bogunovic I, Mesic M, Zgorelec Z, Jurisic A, Bilandzija D (2014) Spatial variation of soil nutrients on sandy-loam soil. Soil Tillage Res 144:174–183. https://doi.org/10.1016/j.still.2014.07.020
Chakrabarti P (1995) Evolutionary history of the coastal quaternaries of the Bengal Plain, India. Proc Indian National Sci Acad 61:343–354
Datta D, Deb S (2017) Forest structure and soil properties of mangrove ecosystems under different management scenarios: experiences from the intensely humanized landscape of Indian Sunderbans. Ocean Coast Manag 140:22–33. https://doi.org/10.1016/j.ocecoaman.2017.02.022
Datta A, Basak N, Chaudhari SK, Sharma DK (2015) Soil properties and organic carbon distribution under different land uses in reclaimed sodic soils of North-West India. Geoderma Reg 4:134–146. https://doi.org/10.1016/j.geodrs.2015.01.006
Datta D, Roy AK, Kundu A, Dutta D, Neogy S (2021) An alternative approach to delineate wetland influence zone of a tropical intertidal mudflat using geo-information technology. Estuar Coast Shelf Sci 253:107308. https://doi.org/10.1016/j.ecss.2021.107308
Deb D, Singh JP, Deb S, Datta D, Ghosh A, Chaurasia RS (2017) An alternative approach for estimating above ground biomass using Resourcesat-2 satellite data and artificial neural network in Bundelkhand region of India. Environ Monit Assess 189:576. https://doi.org/10.1007/s10661-017-6307-6
Dorji T, Odeh IOA, Field DJ, Baillie IC (2014) Digital soil mapping of soil organic carbon stocks under different land use and land cover types in montane ecosystems, Eastern Himalayas. For Ecol Manage 318:91–102. https://doi.org/10.1016/j.foreco.2014.01.003
Eldeiry AA, Garcia LA (2010) Comparison of ordinary kriging, regression kriging, and cokriging techniques to estimate soil salinity using LANDSAT images. J Irrig Drain Eng 136:355–364
Fidêncio PH, Poppi RJ, De Andrade JC (2002) Determination of organic matter in soils using radial basis function networks and near infrared spectroscopy. Anal Chim Acta 453:125–134. https://doi.org/10.1016/S0003-2670(01)01506-9
Fourqurean J, Johnson B, Kauffman JB, Kennedy H, Lovelock C (2014) Field sampling of soil carbon pools in coastal ecosystems. In: Howard J, Hoyt S, Isensee K, Telszewski M, Pidgeon E (eds) Coastal blue carbon: methods for assessing carbon stock and emissions factors in mangroves, tidal salt marshes, and seagrasses. International Union for Conservation of Nature (IUCN), Arlington
Fundisi E, Musakwa W (2017) Built-up area and land cover extraction using high resolution Pleiades satellite imagery for Midrand, in Gauteng Province, South Africa. Int Arch Photogramm Remote Sens Spat Inf Sci. https://doi.org/10.5194/isprs-archives-XLII-2-W7-1151-2017
Gelman F, Binstock R, Halicz L (2012) Application of the Walkley-Black titration for the organic carbon quantification in organic rich sedimentary rocks. Fuel 96:608–610. https://doi.org/10.1016/j.fuel.2011.12.053
Gnanamoorthy P, Selvam V, Ramasubramanian R, Chakraborty S, Pramit D, Karipot A (2019) Soil organic carbon stock in natural and restored mangrove forests in Pichavaram southeast coast of India. Indian J Mar Sci 48:801–808
Guan Y, Bai J, Wang J, Wang W, Wang X, Zhang L, Li X, Liu X (2021) Effects of groundwater tables and salinity levels on soil organic carbon and total nitrogen accumulation in coastal wetlands with different plant cover types in a Chinese estuary. Ecol Indic 121:106969
Harishma KM, Sandeep S, Sreekumar VB (2020) Biomass and carbon stocks in mangrove ecosystems of Kerala, southwest coast of India. Ecol Process 9:31
Haywood BJ, Hayes MP, White JR, Cook RL (2020) Potential fate of wetland soil carbon in a deltaic coastal wetland subjected to high relative sea level rise. Sci Total Environ 711:135185
Howard J, Hoyt S, Isensee K, Pidgeon E, Telszewski M (eds.) (2014) Coastal Blue Carbon: methods for assessing carbon stocks and emissions factors in mangroves, tidal salt marshes, and seagrasses meadows. Conservation International, Intergovernmental Oceanographic Commission of UNESCO, International Union for Conservation of Nature, Arlington

Huang C, David LS, Townshend JRG (2002) An assessment of support vector machines for land cover classification. Int J Remote Sens 23:725–749. https://doi.org/10.1080/01431160110040323
Huo LL, Lv XG, Lin DS (2014) Effect of reclamation on the vertical distribution of SOC in three types of wetland soils. Open J Adv Mater Res 962–965:1386–1391. https://doi.org/10.4028/www.scientific.net/AMR.962-965.1386
IPCC (2021) IPCC fifth assessment report. Intergovernmental panel on climate change. Cambridge University Press, New York
Jiang L, Liang J, Lu X, Hou E, Hoffman FM, Luo Y (2021) Country-level land carbon sink and its causing components by the middle of the twenty-first century. Ecol Process 10:61
Jonsson MN, Hedman AM (2018) Carbon stock assessment of mangrove ecosystems in Batticaloa Lagoon, Sri Lanka, with different degrees of human disturbances. Singap J Trop Geogr 40:199–218. https://doi.org/10.1111/sjtg.12267
Kandasamy K, Rajendran N, Balakrishnan B, Thiruganasambandam R, Narayanasamy R (2021) Carbon sequestration and storage in planted mangrove stands of *Avicennia marina*. Reg Stud Mar Sci 43:101701
Kathiresan K, Kandasamy S, Mullai P (2014) Bioaccumulation of trace elements by *Avicennia marina*. J Coast Life Med 2:888–894. https://doi.org/10.12980/JCLM.2.2014JCLM-2014-0011
Kauffman JB, Donato DC (2012) Protocols for the measurement, monitoring and reporting of structure, biomass and carbon stocks in mangrove forests. In: Front Paper. Center for International Forestry Research. Available via JSTOR. https://www.jstor.org/stable/resrep02318.1. Accessed 19 Jan 2022
Kiranmai GU, Sekhar PR (2016) Estimation of soil organic carbon percentage of mangroves/ wetlands of Visakhapatnam coast, Bay of Bengal, India. J Glob Bios 5:3483–3490
Mendoza-Vega J, Karltun E, Olsson M (2003) Estimations of amounts of soil organic carbon and fine root carbon in land use and land cover classes, and soil types of Chiapas highlands, Mexico. For Ecol Manag 177:191–206. https://doi.org/10.1016/S0378-1127(02)00439-5
Mitra A, Banerjee K (2012) Spatial variation in organic carbon density of mangrove soil in Indian sundarbans. Natl Acad Sci Lett. https://doi.org/10.1007/s40009-012-0046-6
Mitra A, Sengupta K, Banerjee K (2011) Standing biomass and carbon storage of above-ground structures in dominant mangrove trees in the Sundarbans. For Ecol Manag 261:1325–1335
MOEF & CC (2018) Annual Report. http://www.moef.nic.in. Accessed 23 Jan 2022
Mou X, Liu X, Sun Z, Tong C, Huang J, Wan S, Wang C, Wen B (2018) Effects of anthropogenic disturbance on sediment organic carbon mineralization under different water conditions in coastal wetland of a subtropical estuary. Chin Geogr Sci 28:400–410. https://doi.org/10.1007/s11769-018-0956-4
Mountrakis G, Im J, Ogole C (2011) Support vector machines in remote sensing: a review. ISPRS J Photogramm Remote Sens 66:247–259. https://doi.org/10.1016/j.isprsjprs.2010.11.001
Mulamoottil G, Warner BG, McBean EA (eds) (1996) Wetlands: Environmental Gradients, Boundaries, and Buffers. CRC Press, Boca Raton
Nandi G, Neogy S, Roy AK, Datta D (2020) Immediate disturbances induced by tropical cyclone Fani on the coastal forest landscape of eastern India: a geospatial analysis. Remote Sens Appl: Soc Environ 20:100407. https://doi.org/10.1016/j.rsase.2020.100407
Niyogi D (1975) Quaternary Geology of the coastal plain of West Bengal and Orissa. Indian J Earth Sci 2:51–61
OFSDP (2010) Orissa Forestry Sector Development Project Newsletter. http://www.ofsds.in/Publication/Dec2010E.pdf. Accessed 22 Sep 2021
Padua S, Chattopadhayay T, Bandyopadhyay S, Ramchandran S, Jena RK, Ray P, Roy PD, Baruah U, Sah K, Singh S, Ray SK (2018) A simplified soil nutrient information system: study from the North East Region of India. Curr Sci 114:1241–1249. https://doi.org/10.18520/cs/v114/i06/1241-1249
Panda SS, Chaturvedi N, Dhal NK, Rout NC (2013) An assessment of heavy metal accumulation in mangrove species of Bhitarkanika, Odisha, India. Res Plant Biol 3:1–5
Pandey CN, Pandey R (2013) Carbon sequestration in mangroves of Gujarat, India. Int J Botany Res 3:57–70
Phang VXH, Chou LM, Friess DA (2015) Ecosystem carbon stocks across a tropical intertidal habitat mosaic of mangrove forest, seagrass meadow, mudflat and sandbar. Earth Surf Process Landf 40:1387–1400. https://doi.org/10.1002/esp.3745
Rani V, Bijoy Nandan S, Schwing PT (2021) Carbon source characterisation and historical carbon burial in three mangrove ecosystems on the South West coast of India. Catena 197:104980
Robinson TP, Metternicht G (2006) Testing the performance of spatial interpolation techniques for mapping soil properties. Comput Electron Agric 50:97–108. https://doi.org/10.1016/j.compag.2005.07.003
Ross DJ, Tate KR, Scott NA, Feltham CW (1999) Land-use change: effects on soil carbon, nitrogen and phosphorus pools and fluxes in three adjacent ecosystems. Soil Biol Biochem 31:803–813. https://doi.org/10.1023/B:BIOG.0000005324.37711.63
Roy AK, Datta D (2018) Analyzing the effects of afforestation on estuarine environment of river Subarnarekha, India using geospatial technologies and participatory appraisals. Environ Monit Assess 190:645. https://doi.org/10.1007/s10661-018-7030-7
Roy AK, Ghosh PK, Datta D (2020) Typological inventorization and rapid ecological health assessment of the wetlands of Medinipur coastal plain, India. Folia Geogr 62:22–47
Roy AK, Naskar M, Chakraborty T, Neogy S, Datta D (2021) Assessing the impact of aquafarming on landscape dynamics of coastal West Bengal, India using remotely sensed data and spatial metrics. In: Rani M, Seenipandi K, Rehman S, Kumar P, Sajjad H (eds) Remote sensing of ocean and coastal environments. Elsevier, Amsterdam, pp 117–138
Sahu SC, Kumar M, Ravindranath NH (2016) Carbon stocks in natural and planted mangrove forests of Mahanadi Mangrove Wetland, East Coast of India. Curr Sci 110:2253–2260
Schloeder C, Zimmermann NE, Jacobs MJ (2001) Comparison of methods for interpolating soil properties using limited data. Soil Sci Soc Am J 65:470–479. https://doi.org/10.2136/sssaj2001.652470x
Slamet NS, Dargusch P, Aziz AA, Wadley D (2020) Mangrove vulnerability and potential carbon stock loss from land reclamation in Jakarta Bay, Indonesia. Ocean Coast Manag 195:105283. https://doi.org/10.1016/j.ocecoaman.2020.105283
Toru T, Kibret K (2019) Carbon stock under major land use/land cover types of Hades sub-watershed, eastern Ethiopia. Carbon Balance Manag 14:7. https://doi.org/10.1186/s13021-019-0122-z
UNEP (2012) UNEP Year Book 2012: Emerging issues in our global environment. http://www.unep.org. Accessed 20 Aug 2021
Wang J, Song C, Zhang J, Wang L (2014) Temperature sensitivity of soil carbon mineralization and nitrous oxide emission in different ecosystems along a mountain wetland-forest ecotone in the continuous permafrost of Northeast China. Catena 121:110–118. https://doi.org/10.1016/j.catena.2014.05.007
White JG, Welch RM, Norvell WA (1997) Soil zinc map of the USA using geostatistics and geographic information systems. Soil Sci Soc Am J 61:185–194. https://doi.org/10.2136/sssaj1997.03615995006100010027x
Wuest SB (2009) Correction of bulk density and sampling method biases using soil mass per unit area. Soil Sci Soc Am J 73:312–316. https://doi.org/10.2136/sssaj2008.0063
Xie Y, Chen T, Lei M, Yang J, Guo Q, Song B, Zhou X (2011) Spatial distribution of soil heavy metal pollution estimated by different interpolation methods: Accuracy and uncertainty analysis. Chemosphere 82:468–476. https://doi.org/10.1016/j.chemosphere.2010.09.053
Yu J, Wang Y, Li Y, Dong H, Zhou D, Han G, Wu H, Wang G, Mao P, Gao Y (2012) Soil organic carbon storage changes in coastal wetlands of the modern Yellow River Delta from 2000–2009. Biogeosciences 9:2325–2331. https://doi.org/10.5194/bgd-9-1759-2012

Publisher's Note